arXiv:astro-ph/0204127v1 8 Apr 2002

Deuterated molecules as a probe of ionization fraction in dense interstellar clouds

P. Caselli

Osservatorio Astrofisico di Arcetri, Largo E. Fermi 5, I-50125 Firenze, Italy;

caselli@arcetri.astro.it

Abstract

The ionization degree $x(e)$ ($= n(e)/n(\mathrm{H_2})$, with $n(e)$ and $n(\mathrm{H_2})$ the electron and $\mathrm{H_2}$ number density, respectively) plays a key role in the chemical and dynamical evolution of interstellar clouds. Gas phase ion–molecule reactions are major chemical routes to the formation of interstellar molecules. The time scale for ambipolar diffusion of neutrals across field lines is proportional to the ionization degree, which therefore is a crucial parameter in determining the initial conditions which precede the collapse to form a star. A direct measure of $x(e)$ is hindered by the difficulty of observing $\mathrm{H_3^+}$ and $\mathrm{H_3O^+}$, two of the most abundant molecular ions, and atomic species with low ionization potentials, such as atomic carbon and metals, which may be the main repositories of positive charge.

Deuterium fractionation in molecular ions, in particular $\mathrm{HCO^+}$, has been extensively used to estimate the degree of ionization in molecular clouds. This paper reviews recent work on ionization degree in homogeneous clouds. We will show that the $N(\mathrm{DCO^+})/N(\mathrm{HCO^+})$ column density ratio furnishes a measurement of $x(e)$ only in regions where CO is not significantly depleted, thus in the outer skirts of dense cloud cores. To probe $x(e)$ deep inside the clouds, one has to gauge deuterium enhancement in molecular ions with parent species not affected by depletion (e.g. $\mathrm{N_2H^+}$), and rely on chemical models which take into account the cloud density structure. Unlike $N(\mathrm{DCO^+})/N(\mathrm{HCO^+})$, the $N(\mathrm{N_2D^+})/N(\mathrm{N_2H^+})$ column density ratio is predicted to considerably increase with core evolution (and/or the amount of CO depletion), reaching large values ($\gtrsim 0.2$) in cloud cores on the verge of forming a star.

Keywords: deuterium fractionation, dust, ionization degree, interstellar clouds, interstellar molecules, star formation

1 Introduction

The ionization fraction $x(e)$ of a dense interstellar cloud plays a fundamental role in chemical reaction schemes for molecular formation (e.g. Herbst & Klemperer 1973; Oppenheimer & Dalgarno 1974). A knowledge of $x(e)$ also furnishes information on the ionization rate and thus on the sources which heat and ionize the gas. Moreover, the degree of ionization controls the coupling of the cloud to the magnetic field, and thus regulates the rate of star formation. This is due to the process of ambipolar diffusion (Mestel & Spitzer 1956), whereby the neutral particles contract relative to the ionized component which is tied to the field lines. If the magnetic field threading the dense gas is sufficiently large to prevent immediate collapse, ambipolar diffusion of neutrals across field lines can lead to a situation where a dense core of gas is gravitationally unstable. The time scale for ambipolar diffusion is proportional to the ionization degree (e.g. Spitzer 1978; Shu et al. 1987). Therefore our understanding of the physical processes and the dynamics of interstellar clouds requires a knowledge of electron and ion abundances.

In the theoretical determination of the degree of ionization we run into several sources of uncertainty, including the poorly known cosmic ray flux and metal depletion within the cores, the penetration of UV radiation into regions of high visual extinction due to cloud inhomogeneities, and the proximity to strong X–ray emitters (Caselli 2000; Caselli & Walmsley 2000). A direct measure of electron abundances is hindered by the difficulty of observing H_3^+ (McCall et al. 1999) and H_3O^+ (Phillips et al. 1992; Goicoechea & Cernicharo 2001), two of the most abundant molecular ions in dense clouds, and atomic species with low ionization potential, such as atomic carbon and metals, which may be the main repositories of positive charge. Rather, indirect determination of $x(e)$ through the estimate of molecular column densities sensitive to electron densities and the application of chemical models are used.

Observations of deuterated molecular ions and deuterium fractionation estimates represent a powerful tool to measure the ionization degree (Wootten et al. 1979; Guélin et al. 1982; Dalgarno & Lepp 1984; Caselli et al. 1998; Williams et al. 1998). In fact, using a simple steady state chemical model it is easy to show that the $[DCO^+]/[HCO^+]$

abundance ratio is inversely proportional to $x(e)$ (Sect. 2). Therefore it is tempting to use the observed $N(\mathrm{DCO^+})/N(\mathrm{HCO^+})$ column density ratio to infer $x(e)$. However, there are several caveats to this simple picture, including a varying amount of depletion and molecular abundances along the line of sight (Sect. 2), and the existence of sharp density and temperature gradients (Sect. 3). We will discuss these caveats and show that in regions of high CO depletion $N(\mathrm{DCO^+})/N(\mathrm{HCO^+})$ cannot be used to estimate $x(e)$, because it is tracing conditions outside the depleted core. Instead, other molecular ion column density ratios of the deuterated to nondeuterated form (in particular $N(\mathrm{N_2D^+})/N(\mathrm{N_2H^+})$), help in better constraining the ionization fraction in high density regions, where depletion is more effective.

2 Electron fraction estimates in homogeneous clouds

The formation of deuterated molecules starts with the isotope exchange reaction (Watson 1976):

$$\mathrm{H_3^+ + HD} \rightleftharpoons \mathrm{H_2D^+ + H_2}, \tag{1}$$

which is exothermic by an amount $\Delta E/k = 230$ K (e.g. Millar et al. 1989). At the low temperatures typical of dense interstellar clouds, the reverse of reaction (1) is inhibited and the $[\mathrm{H_2D^+}]/[\mathrm{H_3^+}]$ abundance ratio becomes much larger than the interstellar [D]/[H] ratio of 1.5×10^{-5} (Linsky et al. 1995). The deuterium enhancement in $\mathrm{H_3^+}$ is limited by the rate at which electrons and neutrals destroy $\mathrm{H_2D^+}$. Any increase of the $\mathrm{H_2D^+/H_3^+}$ abundance ratio due to reaction (1) is reflected in other species formed through reactions with $\mathrm{H_3^+}$, such as $\mathrm{HCO^+}$. This can be easily shown by considering a simple chemical model with eight ingredients ($\mathrm{H_2}$, CO, HD, $\mathrm{H_3^+}$, $\mathrm{H_2D^+}$, $\mathrm{DCO^+}$, $\mathrm{HCO^+}$, and electrons). Besides reaction (1), the following scheme is operative:

$$\mathrm{H_3^+ + CO} \rightarrow \mathrm{HCO^+ + H_2} \tag{2}$$

$$\mathrm{H_2D^+ + CO} \rightarrow \mathrm{DCO^+ + H_2} \tag{3}$$

$$\mathrm{H_3^+} + e \rightarrow \textit{products} \tag{4}$$

$$H_2D^+ + e \rightarrow products \quad (5)$$

$$HCO^+ + e \rightarrow CO + H \quad (6)$$

$$DCO^+ + e \rightarrow CO + D. \quad (7)$$

The rate equations governing the abundance of $H_2D^+(n(H_2D^+))$, $DCO^+(n(DCO^+))$ and HCO^+ $(n(HCO^+))$ are:

$$\frac{dn(H_2D^+)}{dt} = k_1 n(H_3^+)n(HD) - k_3 n(H_2D^+)n(CO) - \beta_5 n(H_2D^+)x(e) \quad (8)$$

$$\frac{dn(DCO^+)}{dt} = k_3 n(H_2D^+)n(CO) - \beta_7 n(DCO^+)n(e) \quad (9)$$

$$\frac{dn(HCO^+)}{dt} = k_2 n(H_3^+)n(CO) - \beta_6 n(HCO^+)n(e) \quad (10)$$

At steady state,

$$n(H_2D^+) = \frac{k_1 n(H_3^+)n(HD)}{k_3 n(CO) + \beta_5 n(e)} \quad (11)$$

$$n(DCO^+) = \frac{k_3 n(H_2D^+)n(CO)}{\beta_7 n(e)} \quad (12)$$

$$n(HCO^+) = \frac{k_2 n(H_3^+)n(CO)}{\beta_6 n(e)}, \quad (13)$$

so that, assuming $\beta_7 = \beta_6$ (Lee et al. 1996) and $k_3 = 1/3\ k_2$ (because H_2D^+ can also transfer one of the two protons to CO, thus producing HCO^+ at a rate two times larger than that for DCO^+ production),

$$R_D \equiv \frac{n(DCO^+)}{n(HCO^+)} = \frac{1}{3}\frac{n(H_2D^+)}{n(H_3^+)} = \frac{1}{3}\frac{k_1 n(HD)}{k_3 n(CO) + \beta_5 n(e)}. \quad (14)$$

Substituting numerical factors in eqn. 14 (see Caselli et al. 1998), assuming a kinetic temperature $T = 10$ K and a CO fractional abundance $x(CO) = 9.5\times10^{-5}$ (Frerking et al. 1982), we obtain a simple analytical expression which allow us to directly estimate $x(e)$ $(= n(e)/n(H_2))$ once R_D is known from observations:

$$\frac{x(e)}{10^{-7}} \simeq \frac{0.27}{R_D} - 1.9. \quad (15)$$

Equation (15), obtained for illustrative purposes, is a very rough way to estimate the electron fraction in dense clouds, because several important "complications" have been neglected in deriving it. First of all, eqn. (15) does not take into account the presence in

the gas phase of other neutral species, besides CO, which contribute to the destruction of H_2D^+. In particular, atomic oxygen is predicted to be abundant in the gas phase (e.g. Lee et al. 1996; Caselli et al. 1998, 2001b) and recent ISO observations have confirmed this (e.g. Caux et al. 1999). This has the effect of increasing the second term in the right hand side of eqn. (15) by a factor of a few. Secondly, infrared and millimeter observations towards dense and cold clouds have established that a significant fraction of gaseous CO condenses onto dust grain surfaces (Sect. 2.1), so that in eqn. (15) one should use $x(\mathrm{CO})/f_\mathrm{D}$, where $1/f_\mathrm{D}$ is the fraction of CO in the gas phase. The second term in eqn. (15) should thus explicitly include f_D and $x(\mathrm{O})$, e.g.:

$$\frac{x(e)}{10^{-7}} \simeq \frac{0.27}{R_\mathrm{D}} - 1.9\left[\frac{1}{f_\mathrm{D}} + \frac{x(\mathrm{O})/f'_\mathrm{D}}{10^{-4}}\right]. \tag{16}$$

The depletion factor of atomic oxygen, f'_D, appears to be significantly less than f_D (in the center of L1544, $f'_\mathrm{D} \sim 2$–3, whereas $f_\mathrm{D} \sim 1000$; Caselli et al. 2001b), although direct observational determinations are not easy (e.g. Caux et al. 1999). Another problem with eqns. (15) and (16) is that they only furnish an average value of $x(e)$ along the line of sight, with no clues on the variations of $x(e)$ inside the core which requires a knowledge of the density and abundance gradients (Sect. 3). Finally, several simplifications have been made in the chemical scheme (1) - (7), by neglecting important ingredients in the electron balance of dense clouds, including recombination of atomic and molecular ions on negatively charged dust grains (Draine & Sutin 1987), refractory metals (although significantly depleted; see Sect. 3.1), and the presence of atomic deuterium (Dalgarno & Lepp 1984) which somewhat increases the deuterium fractionation (Anderson et al. 1999).

2.1 The effects of depletion on deuterium fractionation and $x(e)$

For a normal dust to gas ratio and assuming typical dust grains with radius of 0.1 μm, the time scale for a gaseous species to be deposited onto a grain is $t_\mathrm{D} \sim 10^9\sqrt{A_\mathrm{X}}/[Sn(\mathrm{H_2})]$ yr, where A_X is the molecular weight, S is the sticking coefficient and $n(\mathrm{H_2})$ is the number density of molecular hydrogen (e.g. Burke & Hollenbach 1983; van Dishoeck et al. 1993). For unity sticking coefficient (Jones & Williams 1985; Tielens & Allamandola 1987) and

a typical H_2 number density of 10^4–10^5 cm^{-3}, $t_{\rm D} \sim 10^5 - 10^4$ yr, comparable to the dynamical time scale of dense cores. Thus, gas–phase depletion is expected to occur in molecular clouds.

Infrared and millimeter observations have indeed revealed large amounts of CO depletion. In quiescent regions of the Taurus molecular cloud, up to 40% of the total (gas+ice) CO is found in solid form (Chiar et al. 1995). In the densest parts of the IC 5146 molecular cloud, Kramer et al. (1999) found a systematic fall off in the ratio between the $C^{18}O$ column density and the visual extinction, consistent with CO depletion. Large depletion factors ($f_{\rm D} \gtrsim 10$) have been measured towards well known pre–stellar cores: L1544 (Caselli et al. 1999; Sect. 3.1), L1498 (Willacy et al. 1998; Tafalla et al. 2001), L1698B (Jessop & Ward–Thompson 2001), L1495, L1400K, and L1517B (Tafalla et al. 2001).

Following Dalgarno & Lepp (1984), Caselli et al. (1998) have shown that uncertainties on the amount of neutral depletion implies an ambiguous determination of the electron fraction (see their eqn. (3) and Tab. 7). Thus, it is extremely important to estimate $f_{\rm D}$ from observations before attempting any $x(e)$ measurement. In fact, decreased fractional abundances of CO and other neutral species causes a drop in the H_2D^+ and H_3^+ destruction rates, and a rise in the H_2D^+ abundance (via reaction 1) due to the larger H_3^+ abundance. The net result is more efficient deuterium fractionation (see eq. 14). Large values in the observed $R_{\rm D}$ and the use of eqn. (15), which does not account for CO depletion, will give erroneously low $x(e)$ values (note that eqn. (15) cannot account for $R_{\rm D} \geq 0.07$).

To see how the electron fraction is affected by the depletion of neutrals, we consider a "zero–order" analysis, using eqn. (13), generalized to a generic neutral species m ($x(m) \simeq x({\rm CO}) + x({\rm O})$):

$$x(m{\rm H}^+) \quad = \quad \frac{k_m x({\rm H}_3^+) x(m)}{\beta_6 x(e)}, \tag{17}$$

and the steady state equation for $x({\rm H}_3^+)$:

$$x({\rm H}_3^+) \quad = \quad \frac{\zeta / n({\rm H}_2)}{k_m x(m) + \beta_4 x(e)}, \tag{18}$$

where ζ is the cosmic ray ionization rate, $n({\rm H}_2)$ is the H_2 number density, and k_m is the generic rate coefficient for H_3^+ destruction reactions with m ($k_m \sim 10^{-9}$ cm^3 s^{-1}).

Substituting eqn. (18) into eqn. (17) and solving for $x(e)$, we arrive at a quadratic equation with solution:

$$x(e) = -q\,x(m)[1-\sqrt{(}1+z/x(m))] \quad (19)$$

$$q = \frac{k_m}{2\beta_4} \quad (20)$$

$$z = \frac{4\beta_4\zeta/n(\mathrm{H_2})}{\beta_6 k_m x(m\mathrm{H}^+)}. \quad (21)$$

The square root term in the right hand side of eqn. (19) can be expanded in a binomial series, which, truncated at the first order term, gives:

$$x(e) = q\,z/2 \quad (22)$$

independent of $x(m)$, but inversely dependent on $x(m\mathrm{H}^+)$ (see eqn. 21). This means that the electron fraction tends to increase with freezing out of neutrals, if the amount of m depletion becomes large enough to reduce the $m\mathrm{H}^+$ formation rate, despite of the increased H_3^+ abundance. However, even if CO is completely depleted (see Sect. 2), atomic oxygen may maintain a considerable gas phase abundance even at large densities ($n(\mathrm{H_2}) \gtrsim 10^6$ cm^{-3}; see Sect. 3.1). Thus, in zero–order, CO depletion *alone* will not significantly affect $x(e)$. As we will see in Sect. 3, estimates of f_D are needed anyway to fine–tune chemical models.

2.2 The use of detailed chemical models

There have been several attempts in the past to use either the observed degree of deuterium fractionation (e.g. Guélin et al. 1982; Dalgarno & Lepp 1984) or the abundance of selected molecular ions (de Boisanger et al. 1996), together with chemical models, to determine the electron fraction. Recent improvements in the laboratory measurements of the H_3^+ and $\mathrm{H_2D}^+$ dissociative recombination rates (Larsson et al. 1996; Kokoouline et al. 2001), crucial in chemical models, as well as the increased sensitivity, spectral and angular resolution of millimeter telescopes, have furnished new impetus to refine previous determinations of $x(e)$.

Caselli et al. (1998) used the "New Standard Model" of Lee et al. (1996), modified in order to include simple deuterated species, to reproduce the observed $x(\mathrm{DCO}^+)/x(\mathrm{HCO}^+)$

($\equiv R_{\rm D}$) and $x({\rm HCO^+})/x({\rm CO})$ ($\equiv R_{\rm H}$) abundance ratios and thus to put constraints on $x(e)$ in a sample of low mass cloud cores studied by Butner et al. (1995) with the MWO 4.9m telescope (Texas) and the NRAO 12m antenna. Free parameters in these models are: (i) the depletion factor, $f_{\rm D}$; (ii) the abundance of refractory metals, such as Fe, Mg, and Na, initially present in singly charged atomic form, $x(M^+)$; (iii) the cosmic ray ionization rate, ζ; and (iv) $n({\rm H_2})$. Whereas $f_{\rm D}$ and $n({\rm H_2})$ can be estimated from observations, the other two parameters ($x(M^+)$ and ζ) have to be determined through the comparison between observed quantities and model results, in the same manner as $x(e)$. To better constrain these quantities, two observables ($R_{\rm D}$ and $R_{\rm H}$) were included in the analysis. $x(M^+)$ and ζ were varied to cover the range of observed abundance ratios. Using a least–square method to model–fit the calculated data points, Caselli et al. (1998) found that typical parameters in low mass cloud cores are:

$$\begin{aligned} 10^{-8} &\lesssim x(e) \lesssim 10^{-6} \\ 10^{-18} &\lesssim \zeta({\rm s^{-1}}) \lesssim 10^{-16} \\ 10^{-10} &\lesssim x(M^+) \lesssim 10^{-7}, \end{aligned}$$

with $f_{\rm D}$ between 2 and 5. We note that, although $x(M^+)$ is poorly constrained, the values obtained by Caselli et al. (1998) corroborate the view of Graedel et al. (1982) that metals are highly depleted in dense cloud cores. This is indirectly confirmed by the fact that molecules containing Fe, Mg, and Na have not been discovered in molecular clouds. Given the assumed homogeneity of the dark cloud cores, the deduced ranges in $x(e)$ and ζ may appear too large, unless ionization losses are significant through modest column densities of material. Indeed, theoretical (e.g. Hartquist & Morfill 1983, 1994) and experimental (Fukui & Hayakawa 1981) work have shown that this is possible (see also Caselli 2000).

Similar $x(e)$ values ($10^{-7.5} \lesssim x(e) \lesssim 10^{-6.5}$) have been deduced in another sample of low mass cores by Williams et al. (1998), using the Bergin & Langer (1997) chemical model and new observations of CO, ${\rm H^{13}CO^+}$, and ${\rm DCO^+}$ at the NRAO 12m antenna (in this case, ζ was fixed at 5×10^{-17} s^{-1} and the depletion factor was varied between 2 and 0.8). Applying the same method to more massive cores, Bergin et al. (1999)

found electron abundances within a smaller range, $10^{-7.3} \lesssim x(e) \lesssim 10^{-6.9}$. Only the most massive sources stand out as having the lowest electron abundances, $x(e) < 10^{-8}$, in agreement with the findings of de Boisanger et al. (1996).

3 $x(e)$ in heterogeneous clouds

Dense molecular clouds are heterogeneous and highly clumped. A knowledge of the cloud density structure is necessary to accurately estimate the electron fraction across the core. From submillimeter continuum dust emission, Ward–Thompson et al. (1994) found that the radial density profiles of starless cores, assuming a constant dust temperature, is $n(r) \propto r^{-\alpha}$, with $\alpha \sim 0.4$–1.2 at radii less than ~ 4000 AU (the so–called "flattened region"), and approaches $n(r) \sim r^{-2}$ between ~ 4000 AU and ~ 15000 AU (André et al. 1996, Ward–Thompson et al. 1999). This result has been recently questioned based on model calculations of the dust temperature in pre–stellar cores (Zucconi et al. 2001; Evans et al. 2001), which predict temperature drops from about 14 K at the outer core edges to ~ 7 K at the center. Temperature gradients imply more peaked density profiles, with smaller "flattened" zones and larger central densities, similar to the density structure of cores with stars, typically consistent with power–laws of the form $n(r) \propto r^{-2}$ or $r^{-1.5}$ (Motte & André 2001).

The electron fraction estimates listed in Sect. 2 are based on data with angular resolution of the order of an arc minute, which corresponds to about 0.04 pc at the distance of Taurus and Ophiuchus, where most of the studied cores are located. As a consequence, the density profile cannot be resolved, at least in the central part of the core. To study spatial variations in the ionization degree of a dense cloud core one needs to map (i) the dust continuum emission, to derive the density profile, and (ii) several species (at least CO, HCO^+ and DCO^+, but, as shown in Sect. 3.1, this is not enough) using larger telescopes. So far, a single detailed study of the electron fraction variation in dense cores has been performed (in L1544; Caselli et al. 2001b) and in the next section we will summarize the observations and the data analysis which have been used to estimate $x(e)$ as a function of cloud radius.

3.1 The starless core L1544

3.1.1 Observational results

L1544, a starless core in the Taurus Molecular Cloud, is thought to be in an early stage of the star formation process, with evidences for gravitational collapse and no signs of infrared point sources, indicative of the presence of young stellar objects. Thus, it is a good target to investigate the initial conditions for stellar birth. L1544 has been extensively studied in several high density tracers such as CS, CCS, N_2H^+(Tafalla et al. 1998; Williams et al. 1999; Ohashi et al. 1999) and $C^{17}O$ (Caselli et al. 1999). Important results from these studies indicate that (a) L1544 is surrounded by a low density envelope which is undergoing extended infall, and (b) CO is highly depleted at densities above $\sim 10^5$ cm^{-3}, or inside radii of $\sim$ 6000 AU. The high density core nucleus was however not studied in detail because the observed lines avoided the central region due to freeze out of the selected molecules onto dust grains (as in the case of CO, CS, and CCS), or because the low J transitions (e.g. J = 1–0 for N_2H^+) observed are affected by absorption in the low density foreground material.

We have recently undertaken an extensive survey of molecular ions which allowed us to make detailed maps of the L1544 nucleus and investigate gas kinematics as well as determining the electron fraction across the core (Caselli et al. 2001a, 2001b). We mapped $H^{13}CO^+$(1–0), DCO^+(2–1), DCO^+(3–2), N_2H^+(1–0), N_2D^+(2–1), and N_2D^+(3–2) using the IRAM 30m antenna at Pico Veleta. Unlike the CO emission, all the molecular ions trace the dust distribution approximately, indicating that depletion is not so severe as in the case of carbon monoxide (Caselli et al. 1999). There are however differences between different tracers and this is evident in Fig.1, where the half maximum contours of HCO^+ and N_2H^+ isotopomers are compared. $H^{13}CO^+$ and DCO^+ are more extended than N_2H^+ and N_2D^+. Moreover, HCO^+ and DCO^+ peak slightly but significantly off the dust peak, whereas N_2H^+ follows the dust continuum emission and N_2D^+ traces the *core nucleus*, the future stellar cradle.

The formyl ion, formed through the reaction between CO and H_3^+, can be considered a good CO tracer in high density gas because it has a higher dipole moment than the par-

ent species. Analogously, N_2H^+ can be considered a good tracer of the unobservable N_2 . From the morphological differences between the various molecular ions shown in Fig. 1, we deduce that CO is less volatile than N_2, and, consequently, HCO^+ and DCO^+ are less abundant in the core nucleus than N_2H^+ and N_2D^+. This confirms the conclusions of Caselli et al. 1999 who found large degrees of CO depletion towards the L1544 dust peak position and suggests the presence of strong abundance gradients in the core. In particular, toward the dust emission peak, we found different degrees of deuterium fractionation in HCO^+ and N_2H^+ ($N(DCO^+)/N(HCO^+) = 0.04\pm0.02$; $N(N_2D^+)/N(N_2H^+) = 0.24\pm0.02$), which can be reproduced only if differential depletion of molecular species onto dust grains, and density gradients are taken into account in chemical models (models without depletion gradients predict similar degrees of deuterium fractionation in HCO^+ and N_2H^+; e.g. Rodgers & Charnley 2001). As discussed in Caselli et al. (2001b), the greater volatility of N_2 allows N_2H^+ to be more abundant than HCO^+ in the dense and highly CO–depleted central regions of the core. Given that depletion favors deuterium fractionation (see Sect. 2.1), the higher $N(N_2D^+)/N(N_2H^+)$ column density ratio is thus naturally explained as arising from an inner and denser region than that probed by $N(DCO^+)/N(HCO^+)$. From this, one can conclude that $x(e)$ measurements in the center of dense cloud cores, where CO is highly depleted, cannot be based on HCO^+ and DCO^+ observations alone.

3.1.2 Chemical model results

We approximate L1544 by a spherically symmetric cloud with a density profile deduced from 1.3mm continuum dust emission observations (Ward–Thompson et al. 1999): a central density of about 10^6 cm^{-3} inside a radius of 2500 AU, followed by a r^{-2} density fall off until a radius of 10000 AU. We also assumed isothermal conditions with $T = 10$ K, based on recent observations of NH_3(1,1) and (2,2) with the Effelsberg telescope (Tafalla et al. 2001). The temperature drop to 7 K in the central 0.01 pc, predicted by Evans et al. (2001) and Zucconi et al. (2001), which is probably not resolved by the above mentioned NH_3 observations, does not significantly affect our chemical results. Neutral species in the model are H_2, CO, N_2, and atomic oxygen. A fundamental assumption here is that

all gas phase N is in molecular form, and C is in CO. This assumption is validated by the general agreement with the "late time" results of the detailed chemical–dynamical model by Aikawa et al. (2001) applied to L1544. We follow depletion of these species onto dust grains and their desorption due to cosmic ray impulsive heating of the dust, following the procedure of Hasegawa & Herbst (1993). The abundance of $HCO^+$and N_2H^+ are given by the steady state chemical equations using the instantaneous abundances of neutral species. Analogously, the electron fraction $x(e)$ is computed in terms of global estimates for the molecular and metallic ions and using instantaneous abundances of CO, N_2, and O in the gas phase, using a simplified version of the reaction scheme of Umebayashi & Nakano (1990).

The $x(DCO^+)/x(HCO^+)$ and $x(N_2D^+)/x(N_2H^+)$ abundance ratios, R_D, are computed assuming that the deuterated species forms by proton transfer from H_2D^+:

$$R_D = \frac{k_1 x(\mathrm{HD})}{3[\beta_5 x(e) + k_m x(m) + k_g x(g)]}. \tag{23}$$

In the above equation, k_1 is the rate coefficient of reaction 1, β_5 is the rate for dissociative recombination of H_2D^+ (reaction 5), k_m is the rate coefficient for H_3^+ (and H_2D^+) destruction with neutral species m, and k_g is the rate for recombination of H_2D^+ on grain surfaces (Draine & Sutin 1987). $x(m)$ is an average over CO, N_2, and O abundances, weighted by the respective depletion factors, and $x(g)$ is the grain abundance by number (computed, together with k_g, using the MNR (Mathis et al. 1977) grain size distribution).

We run several models changing parameters such as the cosmic ray ionization rate (ζ), the CO, N_2, and O binding energies onto grain surfaces (E_D), the lower cut–off radius ($a_{\min}$) in the MRN grain size distribution, and the sticking coefficient (S) which gives the probability for a species colliding with a grain to get adsorbed onto its surface. The "best fit" model, which reproduces the molecular column densities observed towards the L1544 dust peak and best follows the observed column density profiles (see Model 3 in Caselli et al. 2001b), has the following parameters: $\zeta = 6\times10^{-18}$ s^{-1} (a factor of 2 smaller than the standard value, usually adopted in chemical models); $S = 1$ (see e.g. Jones & Williams 1985); $E_D(CO) = 1210$ K, appropriate for polar mantles (Tielens & Allamandola 1987); $E_D(N_2) = 787$ K, 1.5 times smaller than the CO binding energy, as

found in calculations by Sadlej et al. 1995; $E_{\rm D}({\rm O}) = 600$ K, a best fit value (1.3 times smaller than that estimated for polar mantles); $a_{\rm min} = 5{\times}10^{-6}$ cm (5 times larger than the MRN value). Whereas $E_{\rm D}({\rm CO})$, $E_{\rm D}({\rm N_2})$, and S have been fixed to values found in the literature, ζ and $E_{\rm D}({\rm O})$ were allowed to change and in fact they are the two crucial "free" parameters in the model. Assuming that the cosmic ray ionization rate does not change across the cloud, a combination of moderately low ζ and O binding energy is necessary to (i) match the observed ${\rm HCO^+}$ and ${\rm N_2H^+}$ column density profiles, and (ii) keep the deuterium fractionation relatively low in the cloud center and reproduce the observed $N({\rm N_2D^+})/N({\rm N_2H^+})$ and $N({\rm DCO^+})/N({\rm HCO^+})$ column density ratios. Good agreement with observations can also be reached if ζ is decreasing toward the core center, and we are currently exploring this possibility.

Radial profiles of molecular and electron fractional abundances from $r \sim 2500$ AU to $r \sim 10000$ AU are shown in Fig. 2. Here, all the species contributing to the electron fraction are displayed, unlike Fig. 8 of Caselli et al. (2001b), where only observed molecular ions are shown. Several interesting predictions can be based on these profiles: (i) ${\rm HCO^+}$ and ${\rm DCO^+}$ abundances rapidly drop below 4000 AU; (ii) ${\rm H_3O^+}$ becomes the major molecular ion once ${\rm HCO^+}$ starts to drop (in agreement with Aikawa et al. 2001); (iii) CO starts to be highly depleted inside 5000 AU (where the fraction of CO in the solid phase is about 1% of the total "canonical" CO abundance of $9.5{\times}10^{-5}$ (Frerking et al. 1982)) and it is almost totally depleted inside 3000 AU (where 99% of the available CO is frozen onto dust grains); (iv) ${\rm N_2}$, being more volatile than CO, maintains large fractions of ${\rm N_2H^+}$ and ${\rm N_2D^+}$ in the core center, although the ${\rm N_2H^+}$ abundance curve presents a slight fall off at $r \lesssim 3000$ AU; (v) large degrees of deuterium fractionation are present at the core center, where $x({\rm N_2D^+})/x({\rm N_2H^+}) \sim 0.4$, due to the large degree of CO depletion; (vi) *electron fraction* values are a few times 10^{-9} toward the core center and increases to a few times 10^{-8} at the outer edge of the core. The central value of $x(e)$ is a factor of about 6 lower than that deduced from the standard relation between $x(e)$ and ${\rm H_2}$ number density ($x(e) \sim 1.3{\times}10^{-5}\ n({\rm H_2})^{-1/2}$; McKee 1989). The relation we find from the model is:

$$x(e) = 5.2 \times 10^{-6} \times n({\rm H_2})^{-0.56}. \tag{24}$$

Once the electron fraction is known and assuming a balance between the magnetic field force – transmitted to neutrals by ion–neutral collisions – and gravity, the ambipolar diffusion time scale is immediately deduced: $t_{\rm AD} = 2.5{\times}10^{13}\ x(e)$ yr in the case of a cylinder (Spitzer 1978) and $t_{\rm AD} = 3.7{\times}10^{13}\ x(e)$ yr for an oblate spheroid (McKee et al. 1993). The interesting thing is that $t_{\rm AD}$ toward the core center is comparable (within a factor of 2–3) to the free–fall time scale, $t_{\rm ff}$, at densities of about 10^6 cm^{-3}, consistent with the idea that the nucleus of the L1544 core is close to dynamical collapse. Similarly, Umebayashi & Nakano (1990) found $t_{\rm AD}/t_{\rm ff} \sim 4$ in their case 2 (the closest to our model) at $n({\rm H_2}) = 10^6$ cm^{-3}. Note that ${\rm H_3^+}$ closely follows ${\rm N_2H^+}$, whereas metal abundances, which are never primary repositories of positive charges in L1544, are negligible at the core center. The undepleted abundances of metals ($x_i(M) = 10^{-7}$) are about one order of magnitude lower than those measured in diffuse clouds (Morton 1974), as is usual in chemical models of dense clouds (e.g. Herbst & Leung 1989; Graedel et al. 1982; Lee et al. 1986; see also Sect. 2.2). On the other hand, McKee (1989) adopts $x_i(M) = 10^{-6}$ in modeling the ionization in (undepleted) molecular clouds. This leads to electron fractions about an order of magnitude larger than predicted by our model.

3.2 Predictions for dense clouds

The chemical model described in Sect. 3.1.2 can be used to investigate the distribution of electron fraction and molecular ions, including the unobservable ${\rm H_3^+}$ and ${\rm H_3O^+}$, in cores with different masses, density profiles, and different amounts of CO depletion compared to L1544. We will describe (i) the case of a "pivotal core", more centrally concentrated and with larger central densities than L1544, which represents a more massive object (M = 12 M$_\odot$, twice the L1544 mass deduced from the dust emission continuum flux), and perhaps a more evolved stage in the process of star formation; (ii) a "flattened core", with a total mass of $\sim$ 1 M$_\odot$, shallower density profile and smaller amount of CO depletion than L1544, representing a starless low mass core in an earlier phase of evolution.

3.2.1 The "pivotal core"

In the widely used "standard" model of isolated star formation (e.g. Shu et al. 1987), a singular isothermal sphere (SIS; Shu 1977) is considered to be the pivotal state (or starting point) for dynamical cloud collapse. We expect a starless core such as L1544 to evolve toward an even more centrally concentrated density distribution. In this section we analyse the chemical composition and the electron fraction of such a cloud, assuming a sphere with constant density of 10^7 cm^{-3} inside $r_f = 1000$ AU (instead of 2500 AU, as in L1544) and external radius at 15000 AU (as in L1544). The total mass of such an object is 12 $M_\odot$. The chemical parameters are the same as in the "best fit" model described in Sect. 3.1.2.

Results of this more centrally concentrated model are displayed in Fig. 3. The large amount of CO depletion inside 4000 AU produces a sharp drop (or a "hole") in the HCO^+ and DCO^+ abundance profiles. No "hole" is present in N_2D^+, whereas the N_2H^+ abundance profile presents a central "valley" of radius $r \sim 3000$ AU, with a much shallower decline than that of HCO^+ and DCO^+. Inside the N_2H^+ valley, deuterium fractionation becomes so important that $[N_2D^+]/[N_2H^+] \gtrsim 1$ at 1000 AU. H_3^+ more or less follows the N_2H^+ abundance curve, within a factor of 2. Another thing to note is that H_3O^+ is the main ion all across the core[1]. HCO^+ becomes predominant only at the outer edges, where CO depletion is negligible, and where S^+, C^+ and metal ions are also important repositories of positive charge. Therefore, HCO^+ column densities and derived abundances can be used as rough estimates of the electron fraction in the core envelope. At smaller radii, one has to rely on N_2H^+ and N_2D^+ observations. As in the case of L1544, the predicted central $x(e)$ value ($\sim 7\times10^{-10}$) implies an ambipolar diffusion time scale locally similar to the free–fall time scale (see Sect. 3.1.2).

[1]If a larger binding enery for atomic oxygen is used (*e.g.* the typical 800 K, instead of 600 K adopted in our best fit model), HCO^+ is the main ion until a radius of about 4000 AU. At smaller radii, H_3O^+, H_3^+, N_2H^+ and N_2D^+ almost equally contribute to the ionization degree.

3.2.2 Flattened cores

In this case, we use the "typical" radial profile of a pre–stellar core deduced from millimeter observations of dust emission (Ward–Thompson et al. 1994; André et al. 2000; see Sect. 3), with a density profile $n(r) \propto r^{-0.4}$ inside 4000 AU and $n(r) \propto r^{-2}$ at larger radii. The central density, assumed constant inside 1000 AU, is 10^5 cm^{-3}(see right panel in Fig. 4). This profile is similar to four starless cores recently studied by Tafalla et al. (2001), and thus it is representative of starless low mass cores (e.g. Benson & Myers 1989). Indeed, L1544 is an exceptional starless low mass core, because of its large central densities and steep density profiles compared to the majority of the low mass core sample (see also Lee et al. 2001). The observed $C^{17}O$ column density towards the central position is assumed 1×10^{14} cm^{-2}, or six times lower than towards the L1544 molecular peak, based on Ladd et al. (1998) and Tafalla et al. (2001) estimates in similar objects.

The input parameters for the "flattened" core are the same as in the L1544 model and radial abundance profiles are displayed in Fig. 4. The first thing to note is that depletion factors are significantly smaller than in L1544, reaching a maximum of 100 at 1000 AU. HCO^+ and DCO^+ abundances show a shallower drop, and deuterium fractionation is not as effective as in L1544, because of the larger amount of CO in the gas phase (Sect. 2.1). Once again, H_3O^+ is the main molecular ion across the core.

The electron fraction, inside the flattened region ($r \leq 4000$ AU) is about 10^{-8}, about a factor of 4 lower than predicted by the "standard" $x(e) - n(H_2)$ relation (see Sect. 3.1.2). This value of $x(e)$ implies a time–scale for the ambipolar diffusion process of $t_{\rm ad} \simeq 2.5\times10^5$ yr, a factor of two larger than the free–fall time scale $t_{\rm ff}$ at the density of the flattened region (10^5 cm^{-3}). A consequence of this result is that, inside r_f, magnetic fields and ion–neutral coupling are only marginally supporting the core against gravity, so that if no other support is available, the core life time is comparable to its dynamical time scale. This is in contrast with the "standard" model of low mass star formation, where $t_{\rm ad}/t_{\rm ff} \sim 10$ (deduced from the "standard" ionization model of molecular clouds) is used to justify the quasistatic treatment of ambipolar diffusion in the formation of low–mass cores (Shu et al. 1987; Mouschovias 1987). As discussed in Sect. 3.1.2, depletion of metals is the cause of the reduced ionization degree.

3.2.3 Column density profiles

Integrating molecular abundances along the line of sight and convolving with the telescope beam, we can make predictions about column densities and molecular distributions of observable species in the above two model clouds. Fig. 5 shows the column density profiles of the "flattened" and "pivotal" clouds, together with the L1544 results described in Caselli et al. 2001b (assuming the beam of the 30m antenna). The L1544 panels also report observational data (symbols connected by dotted lines) which have been used to put constraints on the chemical model and find the best fitting set of parameters (see Caselli et al. 2001b and Sect. 3.1.2 for more details). We note that the central "valley" in the $C^{17}O$ column density profile becomes more pronounced in the pivotal core, because of the larger amount of CO depletion. The pivotal core also presents a well defined central depression in the HCO^+ and DCO^+ column density profiles, accompanied by a small amount of limb brightening (observed in the $C^{17}O$(1–0) map of L1544; Caselli et al. 1999). The abundance "hole" in HCO^+ and DCO^+ (see Fig. 3) should thus be observable (at the 30m telescope) in more evolved and/or more massive cores.

An interesting result of Fig. 5 is the difference in the N_2D^+ column density and N_2D^+/N_2H^+column density ratio between the three clouds, whereas $N(DCO^+)/N(HCO^+)$ does not significantly change. The flattened core presents the smallest deuterium enhancement in N_2H^+ ($N(N_2D^+)/N(N_2H^+) = 0.085$, at the N_2H^+ column density peak). Indeed, recent observations toward four low mass starless cores (Caselli et al. 2001, in prep.) show marginal detections of N_2D^+ and significantly lower amounts of deuterium fractionation compared to L1544. On the other hand, the pivotal core shows a very sharp N_2D^+ morphology and a central $N(N_2D^+)/N(N_2H^+) \simeq 1$. Thus, the $N(N_2D^+)/N(N_2H^+)$ column density ratio may be a good indicator of core evolution.

4 Discussion and conclusions

Deuterium fractionation in abundant molecular ions offers a powerful tool to determine the fractional ionization of molecular clouds. Simple chemical models of homogeneous clouds clearly show the strong relation between the $N(DCO^+)/N(HCO^+)$ column density ratio

and $x(e)$ (e.g. eqn. (15)). Therefore, accurate estimates of $N(\mathrm{DCO^+})$ and $N(\mathrm{HCO^+})$ are the first steps towards an educated $x(e)$ guess. This implies accounting for the optical depth of observed lines and self–absorption effects, which can be accomplished via observations of rare isotopomers (e.g. $\mathrm{D^{13}CO^+}$, $\mathrm{HC^{18}O^+}$, $\mathrm{HC^{17}O^+}$; Caselli et al. 2001b) and/or lines with hyperfine structure (e.g. the $\mathrm{N_2H^+}$ and $\mathrm{N_2D^+}$ rotational lines; Caselli et al. 1995, Gerin et al. 2001). However, the degree of deuterium fractionation is also strongly affected by the depletion of neutral species (mainly CO and O; see Sect. 2.1), so that it is necessary to estimate the amount of CO depletion before attempting $x(e)$ measurements. Using the above observational data as constraints for detailed chemical models of homogeneous clouds, one can determine an average value of $x(e)$ (Sect. 2.2). Typical ionization fractions are (i) between 10^{-8} and 10^{-6} in low mass cores (Caselli et al. 1998), (ii) $10^{-7.3} \lesssim x(e) \lesssim 10^{-6.9}$ in more massive cores (Bergin et al. 1999), and (iii) $< 10^{-8}$ in very massive massive clouds (de Boisanger et al. 1996).

The study of spatial variations in the ionization degree of a dense cloud requires (i) maps of the dust continuum emission (or the dust extinction; e.g. Lada et al. 1994; Alves et al. 2001), to derive the density profile, and (ii) several molecular line maps (CO, $\mathrm{HCO^+}$, $\mathrm{DCO^+}$, $\mathrm{N_2H^+}$, $\mathrm{N_2D^+}$), to put constraints on the chemistry. In fact, as established from the recent study of L1544 (Caselli et al. 2001a, 2001b) and other starless cores (Tafalla et al. 2001), dense cloud cores experience a phase of strong molecular abundance gradients which can be reproduced by chemical models only by taking into account the density structure, gas phase depletion, and different binding energies of neutral species onto dust grain surfaces (see also Aikawa et al. 2001). In the case of L1544, CO is highly depleted at densities above about 10^5 cm^{-3}, causing the abundance of related species such as $\mathrm{HCO^+}$ and $\mathrm{DCO^+}$ to rapidly drop in the inner parts of the core. This explains the relatively low $N(\mathrm{DCO^+})/N(\mathrm{HCO^+})$ column density ratio ($\simeq 0.04$) observed towards the L1544 dust emission peak. On the other hand, the more volatile $\mathrm{N_2}$ maintains a rich nitrogen chemistry in the gas phase, causing a large deuterium enhancement in $\mathrm{N_2H^+}(N(\mathrm{N_2D^+})/N(\mathrm{N_2H^+}) \simeq 0.24$, toward the same position). Given that $\mathrm{N_2}$ is also precursor of $\mathrm{NH_3}$, large ammonia deuteratium fractionations are expected, and indeed observed by Shah & Wootten (2001) in L1544 and by Tiné et al. (2000) in similar cores.

Inside the "flattened" zone of L1544 ($r_f = 2500$ AU), where the density is $\sim 10^6$ cm^{-3}, we derive an electron fraction of a few times 10^{-9}, implying an ambipolar diffusion time scale locally similar to the free–fall rate, consistent with the idea that the L1544 core is close to dynamically collapse. This is in agreement with the conclusions of Aikawa et al. (2001) who best reproduce observed molecular distributions using *fast* collapse in their dynamical–chemical model. The value we derive for $x(e)$ is about an order of magnitude smaller than the one deduced from the standard relation between $x(e)$ and $n(H_2)$, expected if the electron fraction is due to cosmic ray ionization alone and without depletion (as in McKee 1989).

Our chemical model applied to different types of clouds, predicts an observable increase in the $N(N_2D^+)/N(N_2H^+)$ column density ratio as the core evolves towards steeper density profiles, larger central densities, and more CO–depleted inner regions ($N(N_2D^+)/N(N_2H^+)$ = 0.085, 0.23, and ~ 1 for the flattened core, L1544, and the pivotal core, respectively). On the other hand, the $N(DCO^+)/N(HCO^+)$ ratio does not significantly change (= 0.05, 0.07, and 0.08 for the flattened, L1544, and pivotal cores, respectively). The different deuterium enhancements in HCO^+ and N_2H^+ reflect the cloud density structures, the molecular abundance gradients, and differential depletion of neutral species onto dust grains. HCO^+ and DCO^+ do not trace the inner core regions, and, although the observed $N(DCO^+)/N(HCO^+)$ column density ratio is useful to put constraints on chemical models, the determination of the ionization degree inside the cloud requires observations of N_2H^+ and N_2D^+. These two species (in particular N_2D^+) maintain large abundances at densities $\gtrsim 10^6$ cm^{-3} so that they offer a guide to chemical and physical properties, as well as the dynamical behaviour (see Caselli et al. 2001a), of the high density core nucleus, where the formation of a star will eventually take place. This is extremely important for unveiling the initial conditions in the star formation process, including the fundamental parameter $x(e)$.

Acknowledgements

I am grateful to all my collaborators and, in particular, to Malcolm Walmsley for stimulating discussions. I thank the referees for their useful comments and suggestions, and I acknowledge support from ASI Grant 98-116 as well as from the MURST project

"Dust and Molecules in Astrophysical Environments".

References

Aikawa, Y., Ohashi, N., Inutsuka, S., Herbst, E., Takakuwa, S., 2001. Molecular evolution in collapsing prestellar cores. ApJ. 552, 639B653.

Alves, J.F., Lada, C.J., Lada, E.A., 2001. Internal structure of a cold dark molecular cloud inferred from the extinction of background starlight. Nature. 409, 159B161.

Anderson, I.M., Caselli P., Haikala, L.K., Harju, J., 1999. Deuterium fractionation and the degree of ionization in the R Coronae Australis molecular cloud core. A&A. 347, 983B999.

André P., Ward–Thompson, D., Motte, F., 1996. Probing the initial conditions of star formation: the structure of the prestellar core L 1689B. A&A. 314, 625B635.

Benson, P.J., Myers, P.C., 1989. A survey for dense cores in dark clouds. ApJS. 71, 89B108.

Bergin, E.A., Langer, W.D., 1997. Chemical evolution in preprotostellar and protostellar cores. ApJ. 486, 316B328.

Bergin, E.A., Plume, R., Williams, J.P., Myers, P.C., 1999. The Ionization Fraction in Dense Molecular Gas. II. Massive Cores. ApJ. 512, 724B739.

Burke, J.R., Hollenbach, D.J., 1983. The gas-grain interaction in the interstellar medium - Thermal accommodation and trapping. ApJ. 265, 223B234.

Butner, H.M., Lada, E.A., Loren, R.B., 1995. Physical properties of dense cores: DCO^+ observations. ApJ. 448, 207B225.

Caselli, P., 2000. The fractional ionization in molecular cloud cores. In: Minh, Y.C., van Dishoeck, E.F. (Eds.), Astrochemistry: From Molecular Clouds to Planetary Systems, Proceedings of IAU Symposium 197. Astronomical Society of the Pacific, pp. 41B50.

Caselli, P., Myers, P.C., Thaddeus, P., 1995. Radio-astronomical spectroscopy of the hyperfine structure of N_2H^+. ApJ. 455, L77BL80.

Caselli, P., Walmsley, C.M., 2000. Ionization and chemistry in the dense interstellar

medium. In: Montmerle, T., André, P. (Eds.), From Darkness to Light, ASP Conference Series, in press.

Caselli, P., Walmsley, C.M., Tafalla, M., Dore, L., Myers, P.C., 1999. CO depletion in the starless cloud core L1544. ApJ. 523, L165BL169.

Caselli, P., Walmsley, C.M., Zucconi, A., Tafalla, M., Dore, L., Myers, P.C., 2001a. Molecular ions in L1544. I. Kinematics. ApJ. in press.

Caselli, P., Walmsley, C.M., Zucconi, A., Tafalla, M., Dore, L., Myers, P.C., 2001b. Molecular ions in L1544. II. The ionization degree. ApJ. in press.

Caselli, P., Walmsley, C.M., Terzieva, R., Herbst, E., 1998. The ionization fraction in dense cloud cores. ApJ. 499, 234B249.

Caux, E., Ceccarelli, C., Castets, A., Vastel, C., Liseau, R., Molinari, S., Nisini, B., Saraceno, P., White, G. J., 1999. Large atomic oxygen abundance towards the molecular cloud L1689N. A&A. 347, L1-L4.

Chiar, J.E., Adamson, A.J., Kerr, T.H., Whittet, D.C.B., 1995. High-resolution studies of solid CO in the Taurus dark cloud: characterizing the ices in quiescent clouds. ApJ. 455, 234B243.

Dalgarno, A., Lepp, S., 1984. Deuterium fractionation mechanisms in interstellar clouds. ApJ. 287, L47BL50.

de Boisanger, C., Helmich, F.P., van Dishoeck, E.F., 1996. The ionization fraction in dense clouds. A&A. 310, 315B327.

Draine, B.T., Sutin, B., 1987. Collisional charging of interstellar grains. ApJ. 320, 803B817.

Evans, N.J., II, Rawlings, J.M.C., Shirley, Y.L., Mundy, L.G., 2001. Tracing the mass during low-mass star formation. II. Modeling the submillimeter emission from preprotostellar cores. ApJ. 557, 193B208.

Frerking, M.A., Langer, W.D., Wilson, R.W., 1982. The relationship between carbon monoxide abundance and visual extinction in interstellar clouds. ApJ. 262, 590B605.

Fukui, Y., Hayakawa, S., 1981. Interactions of cosmic rays with molecular clouds. In: International Cosmic Ray Conference, 17th, Conference Papers. Volume 2. Gif-sur-Yvette, Essonne, France, Commissariat a l'Energie Atomique, pp. 226B228.

Gerin, M., Pearson, J.C., Roueff, E., Falgarone, E., Phillips, T.G., 2001. Determination of the hyperfine structure of N_2D^+. ApJ. 551, L193BL197.

Goicoechea, J.R., Cernicharo, J., 2001. Far-Infrared detection of H_3O^+ in Sagittarius B2. ApJ. 554, L213BL216.

Graedel, T.E., Langer, W.D., Frerking, M.A., 1982. The kinetic chemistry of dense interstellar clouds. ApJS. 48, 321B368.

Guelín, M., Langer, W.D., Wilson, R.W., 1982. The state of ionization in dense molecular clouds. A&A. 107, 107B127.

Hasegawa, T.I., Herbst, E., 1993. New gas–grain chemical models of quiescent dense interstellar clouds - The effects of H_2 tunnelling reactions and cosmic ray induced desorption. MNRAS. 261, 83B102.

Hartquist, T.W., Morfill, G.E., 1983. Evidence for the stochastic acceleration of cosmic rays in supernova remnants. ApJ. 266, 271B275.

Hartquist, T.W., Morfill, G.E., 1994. Cosmic ray diffusion at energies of 1 MeV to 10^5 GeV. Ap&SS. 216, 223B234.

Herbst, E., Leung, C.M., 1989. Gas–phase production of complex hydrocarbons, cyanopolyynes, and related compounds in dense interstellar clouds. ApJS. 69, 271B300.

Herbst, E., Klemperer, W., 1973. The formation and depletion of molecules in dense interstellar clouds. ApJ. 185, 505B534.

Jones, A.P., Williams, D.A., 1985. Time-dependent sticking coefficients and mantle growth on interstellar grains. MNRAS. 217, 413B421.

Kokoouline, V., Greene, C.H., Esry, B.D., 2001. Mechanism for the destruction of H_3^+ ions by electon impact. Nature. 412, 891B894.

Lada, C.J., Lada, E.A., Clemens, D.P., Bally, J., 1994. Dust extinction and molecular

gas in the dark cloud IC 5146. ApJ. 429, 694B709.

Ladd, E.F., Fuller, G.A., Deane, J.R., 1998. $C^{18}O$ and $C^{17}O$ observations of embedded young stars in the Taurus Molecular Cloud. I. Integrated intensities and column densities. ApJ. 495, 871B890.

Larsson, M., Lepp, S., Dalgarno, A., et al., 1996. Dissociative recombination of $H_2D^+$and the cosmic abundance of deuterium. A&A. 309, L1BL3.

Lee, H.-H., Bettens, R.P.A., Herbst, E., 1996. Fractional abundances of molecules in dense interstellar clouds: A compendium of recent model results. A&AS. 119, 111B114.

Lee, C.W., Myers, P.C., Tafalla, M., 2001. A survey for infall motions toward starless cores. II. CS(2–1) and N_2H^+(1–0) mapping observations. ApJS. in press.

Linsky, J.L., Diplas, A., Wood, B.E., Brown, A., Ayres, T.R., Savage, B.D., 1995. ApJ. 451, 335B351.

Mathis, J.S., Rumpl, W., Nordsieck, K.H., 1977. The size distribution of interstellar grains. ApJ. 217, 425B433.

McCall, B.J., Geballe, T.R., Hinkle, K.H., Oka, T., 1999. Observations of H_3^+ in dense molecular clouds. ApJ. 522, 338B348.

McKee, C.F., 1989. Photoionization–regulated star formation and the structure of molecular clouds. ApJ. 345, 782B801.

McKee, C.F., Zweibel, E.G., Goodman, A.A., Heiles, C., 1993. Magnetic fields in star-forming regions - Theory. Protostars and Planets III Editors, Eugene H. Levy, Jonathan I. Lunine; Publisher, University of Arizona Press, Tucson, Arizona. 327B366.

Mestel, L., Spitzer, L., Jr., 1956. Star formation in magnetic dust clouds. MNRAS. 116, 503B514.

Millar, T.J., Bennett, A., Herbst, E., 1989. Deuterium fractionation in dense interstellar clouds. ApJ. 340, 906B920.

Morton, D.C., 1974. Interstellar abundances toward zeta Ophiuchi. ApJ. 193, L35-L39.

Motte, F., André, P., 2001. The circumstellar environment of low-mass protostars: A

millimeter continuum mapping survey. A&A. 365, 440B464.

Mouschovias, T.Ch., 1987. Star formation in magnetic interstellar clouds. I - Interplay between theory and observations. II - Basic theory. In: Morfill, G.E., Scholer, M. (Eds.), Physical Processes in Interstellar Clouds. Dordrecht, Reidel. pp. 453B489.

Ohashi, N., Lee, S.W., Wilner, D.J., Hayashi, M., 1999. CCS imaging of the starless core L1544: an envelope with infall and rotation. ApJ. 518, L41BL44.

Oppenheimer, M., Dalgarno, A., 1974. The fractional ionization in dense interstellar clouds. ApJ. 192, 29B32.

Phillips, T.G., van Dishoeck, E.F., Keene, J., 1992. Interstellar H_3O^+ and its relation to the O_2 and H_2O abundances. ApJ. 399, 533B550.

Rodgers, S.D., Charnley, S.B., 2001. Gas–phase production of NHD_2 in L134N. ApJ. 553, 613B617.

Sadlej, J., Rowland, B., Devlin, J.P., Buch, V., 1995. J. Chem. Phys. 102, 4804

Shah, R.Y., Wootten, A., 2001. Deuterated ammonia in galactic protostellar cores. ApJ. 554, 933B947.

Shu, F.H., 1977. Self–similar collapse of isothermal spheres and star formation. ApJ. 214, 488–497.

Shu, F.H., Adams, F.C., Lizano, S., 1987. Star formation in molecular clouds - Observation and theory. ARA&A. 25, 23B81.

Spitzer, L., Jr., 1978, Physical Processes in the Interstellar Medium. New York, Wiley.

Tafalla, M., Mardones, D., Myers, P.C., Caselli, P., Bachiller, R., Benson, P.J., 1998. L1544: A starless dense core with extended inward motions. ApJ. 504, 900B914.

Tafalla, M., Myers, P.C., Caselli, P., Walmsley, C.M., Comito, C., 2001. Sistematic molecular differentiation in starless cores. ApJ. submitted.

Tielens, A.G.G.M., Allamandola, L.J., 1987. Evolution of interstellar dust. In: Hollenbach, D.J., Thronson, H.A., Jr. (Eds.), Interstellar Processes. Dordrecht, Kluwer, pp. 333B376.

Tin; S., Roueff, E., Falgarone, E., Gerin, M., Pineau des Forêts, G., 2000. Deuterium fractionation in dense ammonia cores. A&A. 356, 1039B1049.

Umebayashi, T., Nakano, T., 1990. Magnetic flux loss from interstellar clouds. MNRAS. 243, 103B113.

van Dishoeck, E.F., Blake, G.A., Draine, B.T., Lunine, J.I., 1993. The chemical evolution of protostellar and protoplanetary matter. In: Levi, E.H., Lunine, J.I. (Eds.), Protostars and planets III. Tucson, Univ. Arizona Press, pp. 163B241.

Ward-Thompson, D., Motte, F., André, P., 1999. The initial conditions of isolated star formation - III. Millimetre continuum mapping of pre-stellar cores. MNRAS. 305, 143B150.

Ward–Thompson, D., Scott, P.F., Hills, R.E., André, P., 1994. A submillimetre continuum survey of pre protostellar cores. MNRAS. 268, 276B290.

Watson, W.D., 1976. Interstellar molecule reactions. Rev. Mod. Phys. 48, 513B550.

Willacy, K., Langer, W.D., Velusamy, T., 1998. Dust emission and molecular depletion in L1498. ApJ. 507, L171BL175.

Williams, J.P., Bergin, E.A., Caselli, P., Myers, P.C., Plume, R., 1998. The ionization fraction in dense molecular gas. I. Low-mass cores. ApJ. 503, 689B699.

Williams, J.P., Myers, P.C., Wilner, D.J., di Francesco, J., 1999. A high–rsolution study of the slowly contracting, starless core L1544. ApJ. 513, L61BL64.

Wootten, A., Snell, R., Glassgold, A.E., 1979. The determination of electron abundances in interstellar clouds. ApJ. 234, 876B880.

Zucconi, A., Walmsley, C.M., Galli, D., 2001. The dust temperature distribution in prestellar cores. A&A. 376, 650B662.

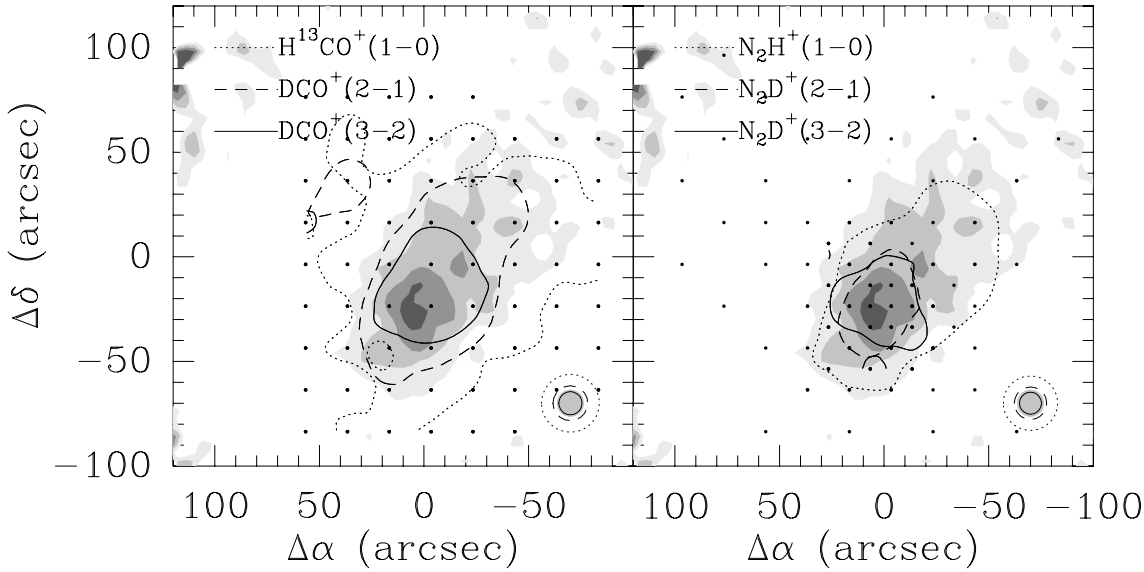

Figure 1: Half maximum contours of integrated intensity maps of (*left*) $H^{13}CO^+$(1–0) (dotted contour), DCO^+(2–1) (dashed), DCO^+(3–2) (thin), and (*right*) N_2H^+(1–0) (dotted), N_2D^+(2–1) (dashed), and N_2D^+(3–2) (thin), overlapped with the 1.3mm continuum dust emission from Ward–Thompson et al. (1999) (gray scale; see Caselli et al. 2001a for details on the observations). Beam sizes at the corresponding frequencies are reported in the bottom right corner. HCO^+ and DCO^+ are more extended than N_2H^+ and N_2D^+, due to the differential depletion of CO and N_2, which causes strong abundance gradients in the core (see text).

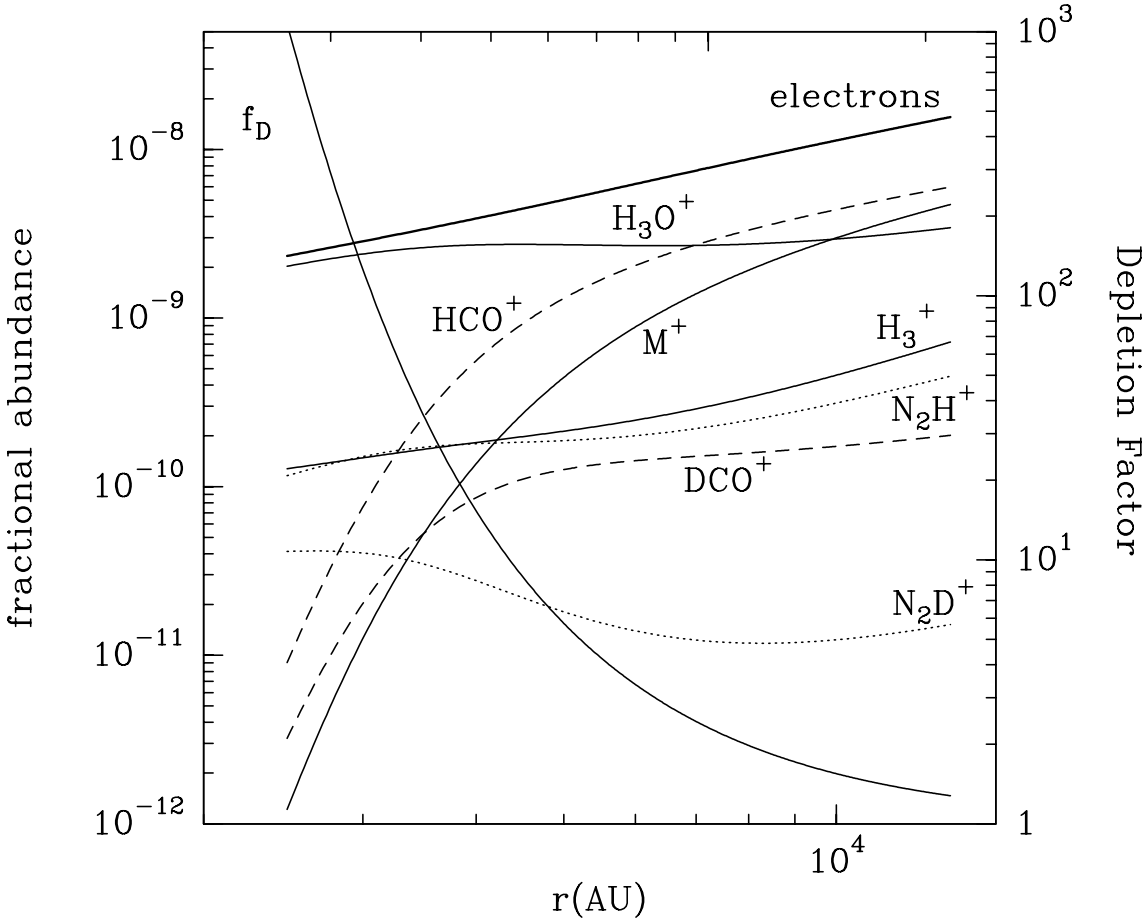

Figure 2: Radial profiles of fractional abundances of electrons, HCO^+, DCO^+, N_2H^+, N_2D^+, H_3O^+, H_3^+ and metal ions (M^+) predicted by the best fit model of Caselli et al. (2001b). f_D is the CO depletion factor. HCO^+ and DCO^+ abundances drastically drop below $r \sim 4000$ AU, whereas no "hole" is present in the N_2D^+ profile. Inside the flattened region, the main molecular ion is H_3O^+. The assumed density profile is based on 1.3mm continuum dust emission observations (Ward-Thompson et al. 1999).

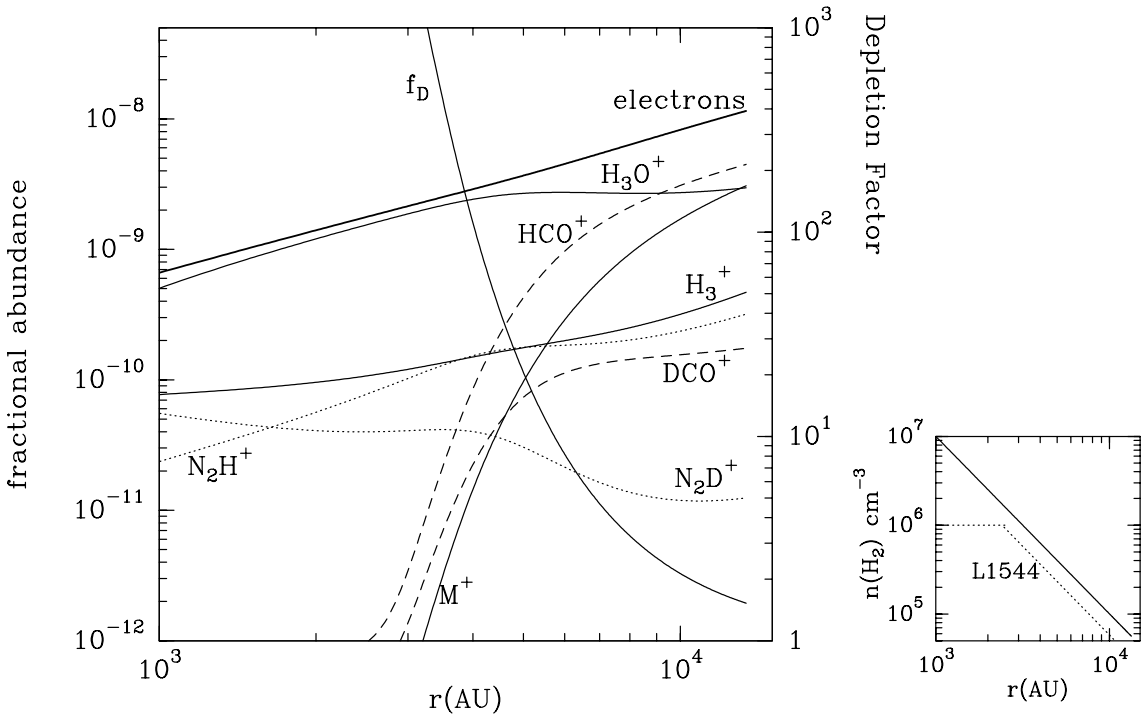

Figure 3: Same as Fig. 2 for a core more centrally concentrated (and eventually more evolved) than L1544. The "flattened" region is 1000 AU in size and has a density of 10^7 cm^{-3}. $f_{\rm D}$ is the CO depletion factor. As in L1544 (see Fig. 2; note the different abscissa scale), HCO^+ and DCO^+ abundances drastically drop below $r \sim 4000$ AU. N_2H^+ gradually declines toward the center, and becomes less abundant than N_2D^+below 2000 AU. The main molecular ion is H_3O^+. The figure on the right shows the density profile of the pivotal core (continuous line), compared to the L1544 profile (dotted curve).

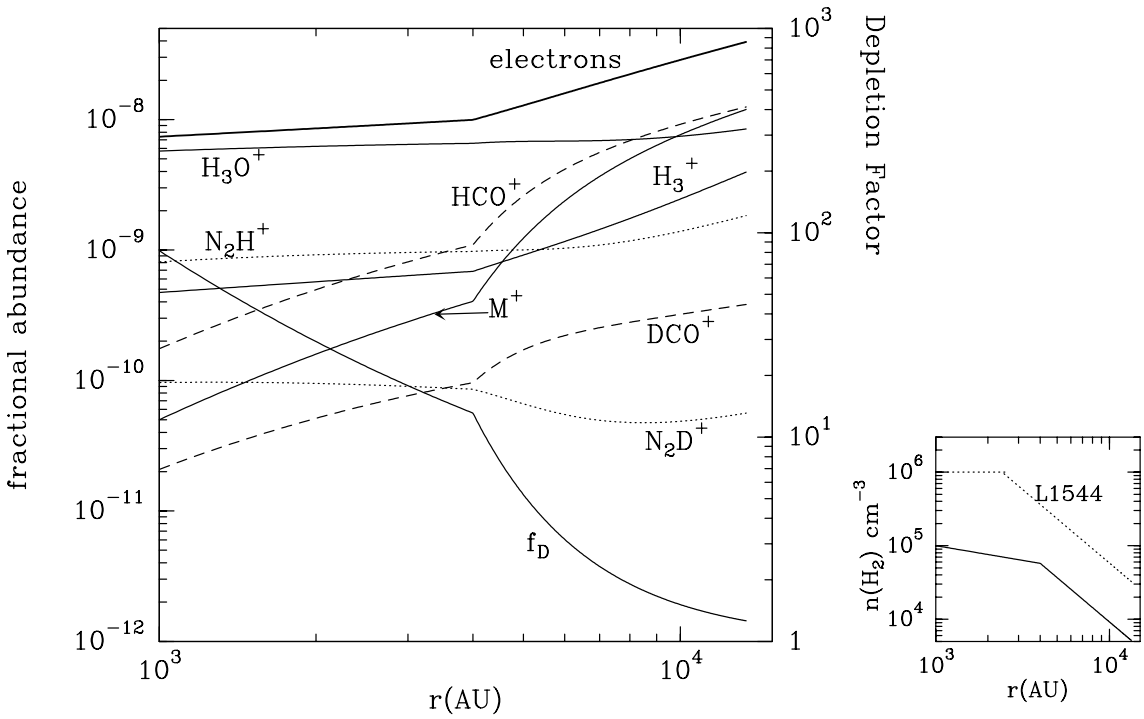

Figure 4: Same as Fig. 2 for a core less dense and less centrally concentrated than L1544, which may represent an earlier stage in the evolution towards the formation of a star. The density drops as $r^{-0.4}$ inside 4000 AU, and as r^{-2} between 4000 and 15000 AU (the assumed cloud radius). The central density is 10^5 cm^{-3} (see right panel). In this case, no "holes" are present in the molecular distribution. Although CO is not significantly depleted, $H_3O^+$is still the main molecular ion at $r \leq 6000$ AU. Deuterium fractionation in HCO^+ and N_2H^+ is constant across the cloud because of the negligible depletion of neutral species.

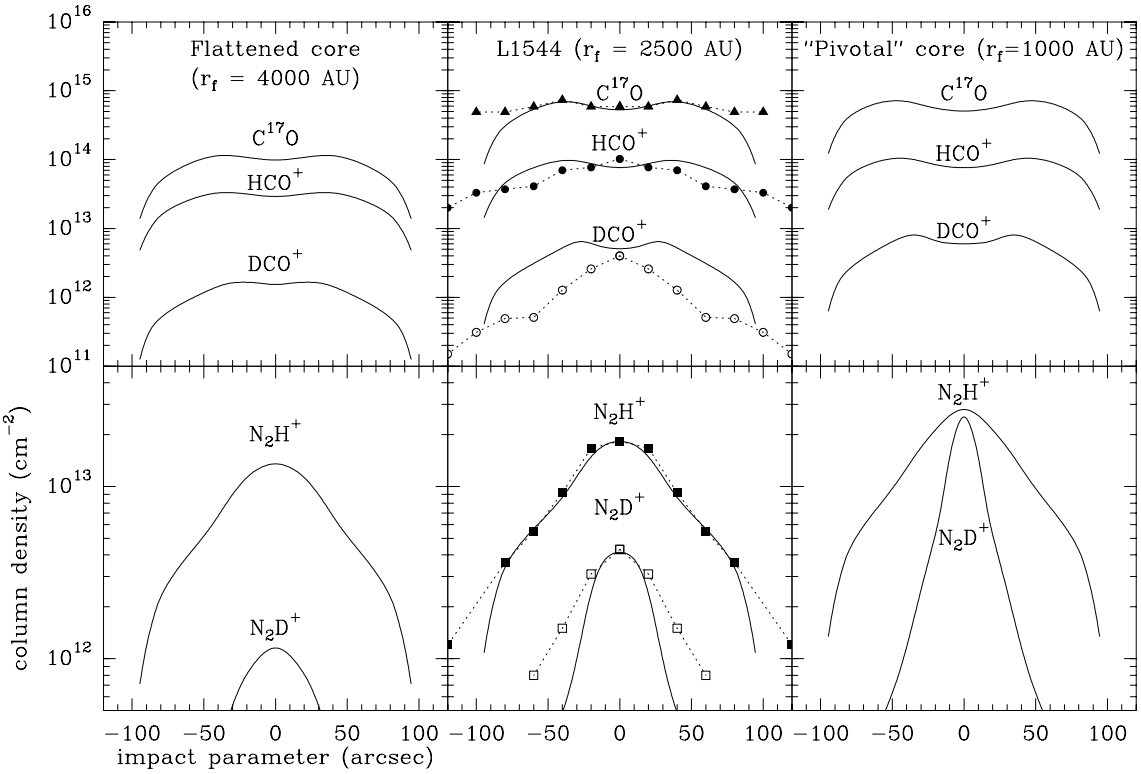

Figure 5: Column density profiles predicted in different dense clouds: (*left*) a flattened cloud (Sect. 3.2.2), representative of low mass cores; (*center*) L1544 (Sect. 3.1) , a low mass starless core on the verge of forming a star. Symbols are observed column densities averaged inside the corresponding bin (Caselli et al. 2001b); (*right*) a "pivotal" cloud (Sect. 3.2.1), representative of more massive cores ($M \sim 10$ $M_\odot$), with higher central density and more centrally concentrated than L1544. The $N(N_2D^+)/N(N_2H^+)$ column density ratio increases with the amount of CO depletion and, probably, the core evolution (see text). Column density profiles have been convolved with the 30m beam, assuming observations of the following transitions: J = 1→0 for $C^{17}O$, HCO^+, DCO^+, and N_2H^+; J = 2→1 for $DCO^+$and N_2D^+.